Jointly Optimized 3D Drone Mounted Base Station Deployment and User Association in Drone Assisted Mobile Access Networks

Xiang Sun, *Member, IEEE*, Nirwan Ansari, *Fellow, IEEE*, and Rafael Fierro, *Senior Member, IEEE*

***Abstract*—In drone assisted mobile networks, a drone mounted base station (DBS) is deployed over a hotspot area to help user equipments (UEs) download their traffic from the macro base station (MBS), thus improving the throughput and spectrum efficiency (SE) of the UEs. Finding the optimal 3D position of the DBS to maximize the overall SE of the UEs in the hotspot area is challenging because the 3D DBS placement and user association problems are coupled together. In this paper, we formulate the problem of jointly optimizing the 3D DBS placement and user association to maximize the overall SE in the context of drone assisted mobile networks. The spectrum efficiency aware DBS placement and user association (STAR) algorithm is designed to decompose the original problem into two subproblems, i.e., user association and DBS placement, and to iteratively solve the two subproblems until the overall SE of the hotspot area cannot be improved further. The performance of STAR is demonstrated via extensive simulations.**

***Index Terms*—Drone base station, spectral efficiency, user association, deployment, drone assisted mobile networks.**

I. Introduction

OWING to quick and flexible deployment, drones have been widely used in various applications, such as public safety [1], disaster relief [2]–[7], content caching [8], and location-based services [9]. In drone assisted mobile access networks, a drone mounted base station (DBS) can be deployed over a hotspot area, which may appear sporadically, to speed up the content delivery rate of users in the hotspot area [10]. For example, a new hotspot might arise after an accident owing to an auto accident, when mobile users begin to stress the access point by downloading and watching related news content. Deploying a DBS over a hotspot area could significantly improve the network performance in terms of throughput or spectrum efficiency (SE) of user equipments (UEs) in the hotspot area [11]–[13]. Specifically, Fig. 1 shows the drone assisted mobile access network architecture, where a DBS is deployed over a hotspot area, and

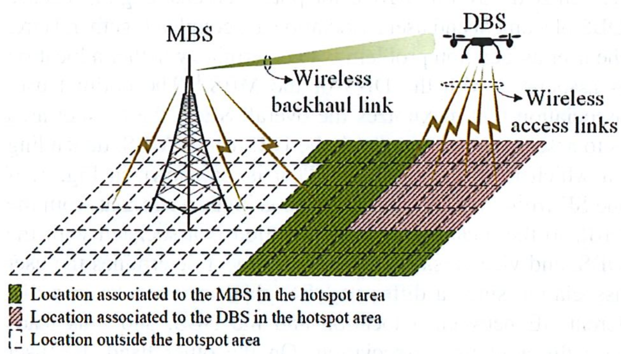

Fig. 1. The drone assisted mobile access network architecture.

so all the UEs can download their requested contents from their macro base station (MBS) via the DBS, which acts as a relay node to receive data from the MBS via the wireless backhaul link and transmit data to the corresponding UEs via the wireless access links. Here, the DBS is operated in the out-of-band mode [14], [15]. That is, the frequency band of the backhaul link is different from the frequency band of the access links, thus avoiding the interference between the access link and the backhaul link. Here, free space optical (FSO) communications is applied as the wireless backhaul solution, and the traditional RF communications is used as the wireless access solution. Note that the data rate achieved by the FSO communications is much higher than the RF communications [16], [17], and so we assume that the bottleneck of transmitting data from the MBS to UEs via the DBS is the wireless access links. Then, the objective of the drone assisted mobile access network is to maximize the overall throughput of the wireless access links between the DBS/MBS and the UEs in the hotspot by determining the 3D position of the DBS. Note that the overall throughput of the UEs in the hotspot area depends on not only the overall SE between the DBS and the UEs but also the amount of bandwidth allocated to the UEs, where the overall SE is determined by the DBS placement method, and the amount of bandwidth assigned to the UEs depends on the bandwidth allocation method. The DBS placement and bandwidth allocation problem cannot be jointly optimized/solved because they are operating under different time scales. That is, in the LTE network setup, bandwidth allocation is conducted in each millisecond [18]; yet, it is impossible and unnecessary to adjust the 3D location of a DBS in each

Manuscript received July 10, 2019; revised November 4, 2019 and December 3, 2019; accepted December 16, 2019. Date of publication December 20, 2019; date of current version February 12, 2020. This work was supported by the National Science Foundation under Awards OIA-1757207 and CNS-1814748. The review of this article was coordinated by Prof. G. Mao. *(Corresponding author: Xiang Sun.)*

X. Sun and R. Fierro are with the Department of Electrical and Computer Engineering, University of New Mexico, Albuquerque, NM 87131 USA (e-mail: sunxiang@unm.edu; rfierro@unm.edu).

N. Ansari is with the Advanced Networking Laboratory, Department of Electrical and Computer Engineering, New Jersey Institute of Technology, Newark, NJ 07102 USA (e-mail: nirwan.ansari@njit.edu).

Digital Object Identifier 10.1109/TVT.2019.2961086

the DBSs have enough energy to hover at least a predefined time period and fly to the nearest charging station for charging their batteries. Under the same scenario, they proposed another 2D DBS placement method to serve more UEs and generate less interference [29] among DBSs. Lyu *et al.* [30] considered the scenario with no available ground BSs in a given area, and so DBSs have to connect to the core network via satellites. Meanwhile, they assumed that the link between a DBS and a UE is LoS, the altitudes of the DBSs are fixed, and all the DBSs have the same coverage size. They derived a 2D DBS placement algorithm to minimize the number of required DBSs, while guaranteeing every UE in the area to be covered by at least one DBS.

In drone assisted mobile access networks, a UE can either be associated with the DBS or the MBS. Thus, jointly optimizing the user association and DBS placement, which is considered by the previous works, can potentially improve the performance of the mobile access network. Our previous works [13], [31] focused on the same topic. In [13], we designed a latency aware DBS placement method to jointly optimize the horizontal location of the DBS and the user association such that the traffic loads of the two base stations are balanced. Yet, the altitude of the DBS is considered to be fixed, and is thus not optimized. In [31], we designed an SE aware DBS placement and user association algorithm to jointly optimize the altitude of the DBS and the user association in order to maximize the SE of the hotspot area. However, the horizontal position of the DBS is always at the center of the hotspot, and so is not optimized. Esrafilian and Gesbert [32] designed a joint user association and DBS placement problem to maximize the SE of the worst UE in the area in the context of uplink communications. However, maximizing the SE of the worst UE is not equivalent to maximizing the overall SE of the UEs in the area. We will provide the performance comparison via extensive simulations in Section V.

III. System Model

A hotspot area is discretized into a number of small locations with the same size. Denote $\mathcal{I}$ as the set of these locations, each indexed by i. Denote h as the altitude of the DBS. Meanwhile, let $l_{ii'}$ be the horizontal distance between location i and location i', where $i, i' \in \mathcal{I}$. Thus, the horizontal distance between the DBS and the UEs in location i is $l_i = \sum_{i'\in\mathcal{I}} x_{i'} l_{ii'}$, where $x_{i'}$ is a binary variable to indicate whether the DBS is deployed over location i' (i.e., $x_{i'} = 1$) or not (i.e., $x_{i'} = 0$). Hence, the 3D distance between the DBS and the UEs in location i can be expressed as

$$d_i = \sqrt{{l_i}^2 + h^2} = \sqrt{\sum\nolimits_{i'\in\mathcal{I}} x_{i'} l_{ii'}^2 + h^2}. \tag{1}$$

A. Pathloss Model Between the DBS and a Location

The wireless propagation channel between the DBS and the UEs in location i can be divided into two scenarios, i.e., the links between the DBS and the UEs in location i with line-of-sight (LoS) connections and those with non-line-of-sight (NLoS) connections [22], [33], [34]. In the NLoS scenario, UEs can still communicate with the DBS, but suffer from much stronger reflections and diffractions [35], [36]. The probability of having LoS between the DBS and the UEs in location i can be modeled as [22]

$$\begin{aligned}\rho_i &= \frac{1}{1+\alpha e^{-\beta(\theta_i-\alpha)}} \\ &= \frac{1}{1+\alpha e^{-\beta\left(\frac{180}{\pi}\arctan\left(\frac{h}{\sum_{i'\in\mathcal{I}} x_{i'} l_{ii'}}\right)-\alpha\right)}},\end{aligned} \tag{2}$$

where θ_i (in degrees) is the elevation angle between the DBS and location i, and α and β are the environmental parameters determined by the environment of the hotspot area (e.g., rural, urban, etc.). Thus, the average pathloss (in dB) between the DBS and the UEs in location i can be estimated as [37], [38]

$$\eta_i^d = 20\log_{10}\left(\frac{4\pi f_c d_i}{c}\right) + \rho_i \xi^{los} + (1-\rho_i)\,\xi^{nlos}. \tag{3}$$

Here, $20\log(\frac{4\pi f_c d_i}{c})$ indicates the free space pathloss (where f_c is the carrier frequency and d_i is the 3D distance between the DBS and location i) and $\rho_i\xi^{los} + (1-\rho_i)\xi^{los}$ is the average additional pathloss (where ξ^{los} and ξ^{nlos} are the average additional pathloss for LoS and NLoS scenario, respectively) between the DBS and the UEs in location i. Here, $\xi^{los} < \xi^{nlos}$.

B. Spectrum Efficiency Model

The UEs in location i can be associated with either the MBS or the DBS in downloading their traffic. However, associating with different base stations may incur different SEs. Here, we provide two models to estimate the SEs of enabling the UEs to download data from the MBS and the DBS, respectively.

1) Spectrum Efficiency Between the DBS and a Location: Denote g_i^d as the channel gain from the DBS to the UEs in location i. Assume that the pathloss is the major factor to determine the channel gain between the DBS and the UEs in location i (i.e., shadowing and fading effects are not considered). Thus, the channel gain g_i^d can be estimated by $g_i^d = 10^{-\frac{\eta_i}{10}}$. Consequently, the SE of transmitting data from the DBS to the UEs in location i can be obtained by

$$\varphi_i^d = \log_2\left(1+\frac{p^d 10^{\frac{-\eta_i^d}{10}}}{\sigma^2}\right), \tag{4}$$

where p^d is the transmission power of the DBS and σ^2 denotes the noise power level.

2) Spectrum Efficiency Between the MBS and a Location: Similarly, the SE of transmitting data from the MBS to the UEs in location i can be obtained by

$$\varphi_i^m = \log_2\left(1+\frac{p^m 10^{\frac{-\eta_i^m}{10}}}{\sigma^2}\right), \tag{5}$$

where p^m is the transmission power of the MBS and η_i^m is the pathloss from the MBS to the UEs in location i.

C. Problem Formulation

In drone assisted mobile access networks, a DBS is placed in a hotspot area $\mathcal{I}$ to help the MBS in delivering traffic to the UEs the first part of the objective function, i.e.,

$\boldsymbol{P3}$:

$$\begin{aligned}&\arg\min_{h} \sum_{i\in\mathcal{A}} w_i \\ &\times \left(\rho_i\left(\xi^{los}-\xi^{nlos}\right)-20\log_{10}\left(\frac{\sum_{i'\in\mathcal{I}} x^*_{i'} l_{ii'}}{\sqrt{\sum_{i'\in\mathcal{I}} x^*_{i'} l^2_{ii'}+h^2}}\right)\right)\\ &\text{s.t.}\quad h^{\min}\le h\le h^{\max},\end{aligned}$$

where $x^*_{i'}$ is the optimal solution of $\boldsymbol{P2}$.

1) Horizontal Location of the DBS: As mentioned before, the horizontal location of the DBS is to derive the optimal solution of $\boldsymbol{P2}$. Here, $\boldsymbol{P2}$ can be transformed into

$$\begin{aligned}&\arg\min_{x_{i'}} \log_{10}\left(\prod_{i\in\mathcal{A}}\left(\sum_{i'\in\mathcal{I}} x_{i'} l_{ii'}\right)^{w_i}\right)\\ \Leftrightarrow\ &\arg\min_{x_{i'}} \quad \sum_{i'\in\mathcal{I}}\left(x_{i'}\prod_{i\in\mathcal{A}}\left(l_{ii'}\right)^{w_i}\right)\\ &\text{s.t.} \quad \sum_{i'\in\mathcal{I}} x_{i'}=1,\\ &\qquad \forall i'\in\mathcal{I},\quad x_{i'}\in\{0,1\}.\end{aligned}$$

It is easy to derive the optimal solution of the transformed problem, i.e.,

$$x^*_{i'}=\begin{cases}1, & i'=i^*.\\ 0, & \text{otherwise.}\end{cases} \tag{15}$$

where i^* is the location such that the products of the distances between the location and other locations in $\mathcal{A}$ is the minimum, i.e., $i^*=\arg\min_{i'\in\mathcal{I}}\{\prod_{i\in\mathcal{A}}(l_{ii'})^{w_i}\}$.

2) Altitude of the DBS: The optimal altitude of the DBS can be obtained by solving $\boldsymbol{P3}$. However, it is non-trivial to solve $\boldsymbol{P3}$ since the objective function is neither convex nor concave. Here, we apply the Projected Gradient Descent method [39] to find the local optimal solution of $\boldsymbol{P3}$. The basic idea of applying Projected Gradient Descent to find the local optimal solution of h is to iteratively move the value of h in the direction of steepest descent, which is defined by the negative of the gradient of the objective function in $\boldsymbol{P3}$. Specifically, define f as the objective function of $\boldsymbol{P3}$, i.e.,

$$\begin{aligned}f(h)=&\sum_{i\in\mathcal{A}} w_i\\ &\times\left(\rho_i\left(\xi^{los}-\xi^{nlos}\right)-20\log_{10}\left(\frac{\sum_{i'\in\mathcal{I}} x^*_{i'} l_{ii'}}{\sqrt{\sum_{i'\in\mathcal{I}} x^*_{i'} l^2_{ii'}+h^2}}\right)\right).\end{aligned} \tag{16}$$

Algorithm 1: $PGD(x^*_{i'})$.

Input: $\mathcal{X}=\{x^*_{i'}|i'\in\mathcal{I}\}$.
Output: The altitude of the DBS h^*.

```
Initialize h^(0) and step size δ^(0).
Calculate f(h^(0)) and ∇f(h^(0)) based on Eq. (16) and
  Eq. (17), respectively.
do
    Update h^(k+1) based on Eq. (18);
    Project h^(k+1) into its feasible set based on (20);
    Calculate f(h^(k+1)) and ∇f(h^(k+1));
    Calculate the step size δ^(k+1) based on (19);
while |f(h^(k+1)) − f(h^(k))| > ε
h* = h^(k+1).
return h*.
```

So, the gradient of f with respect to h is expressed in Eq. (17), shown at the bottom of this page.[2] Thus, the steps of the Projected Gradient Descent method are described as follows:

1) Pick an initial value of h, e.g., $h^{(0)}=\frac{h^{\min}+h^{\max}}{2}$.

2) For each iteration k ($k>0$), update the value of h, i.e.,

$$h^{(k+1)}=h^{(k)}-\delta^{(k)}\nabla f\left(h^{(k)}\right), \tag{18}$$

where $h^{(k)}$ and $h^{(k+1)}$ are the value of h in iteration k and $k+1$, respectively, $\nabla f(h^{(k)})$ is the value of the gradient of f at point $h=h^{(k)}$, and $\delta^{(k)}$ is the step size in iteration k (where $k>0$), which is calculated based on the Barzilai-Borwein method [40], i.e.,

$$\delta^{(k)}=\frac{h^{(k)}-h^{(k-1)}}{\nabla f\left(h^{(k)}\right)-\nabla f\left(h^{(k-1)}\right)}. \tag{19}$$

3) Project the value of $h^{(k+1)}$ into the feasible set, i.e.,

$$h^{(k+1)}=\begin{cases}h^{(k+1)}, & h^{\min}\le h\le h^{\max}.\\ h^{\min}, & h<h^{\min}.\\ h^{\max}, & h>h^{\max}.\end{cases} \tag{20}$$

4) The iteration continues until

$$\left|f\left(h^{(k+1)}\right)-f\left(h^{(k)}\right)\right|\le\varepsilon, \tag{21}$$

where ε is a predefined threshold.

The algorithm of applying Projected Gradient Descent to derive the optimal altitude of the DBS, denoted as $PGD(x^*_{i'})$, is summarized in Algorithm 1.

[2]Note that $\forall h\in[h^{\min},h^{\max}]$, $\nabla f(h)$ always exist as long as at least one location is associated with the DBS, i.e., $\sum_{i\in\mathcal{I}} y^*_i\ge 1$.

$$\nabla f(h)=\sum_{i\in\mathcal{A}} w_i\left(\frac{\frac{180}{\pi}\alpha\beta\left(\xi^{los}-\xi^{nlos}\right)e^{-\beta\left(\frac{180}{\pi}\arctan\left(\frac{h}{\sum_{i'\in\mathcal{I}}x^*_{i'}l_{ii'}}\right)-\alpha\right)}\sum_{i'\in\mathcal{I}}x^*_{i'}l_{ii'}}{\left(\sum_{i'\in\mathcal{I}}x^*_{i'}l^2_{ii'}+h^2\right)\left(1+\alpha e^{-\beta\left(\frac{180}{\pi}\arctan\left(\frac{h}{\sum_{i'\in\mathcal{I}}x^*_{i'}l_{ii'}}\right)-\alpha\right)}\right)^2}+\frac{20}{\ln 10}\frac{h}{\sum_{i'\in\mathcal{I}}x^*_{i'}l^2_{ii'}+h^2}\right) \tag{17}$$

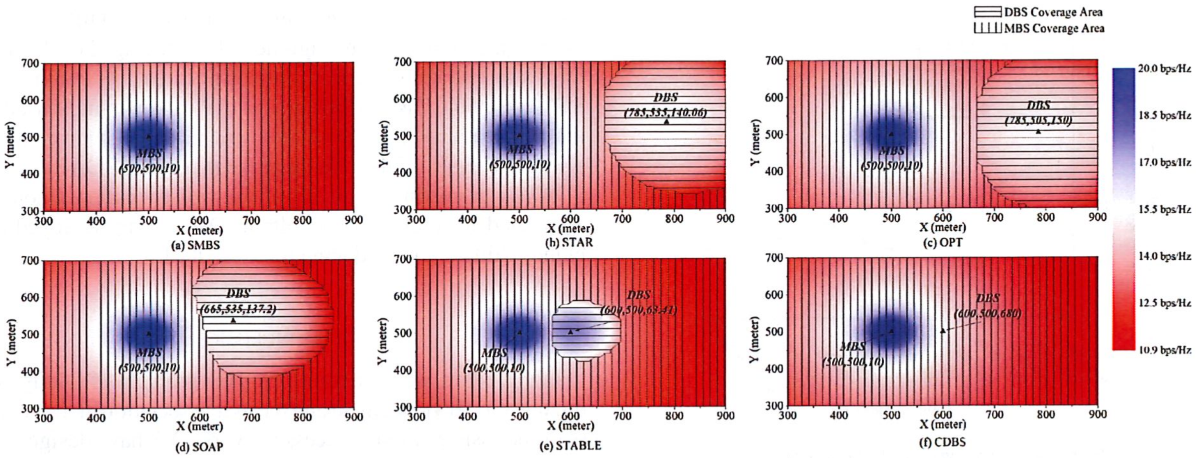

Fig. 2. SE distribution in the hotspot area.

associated locations, i.e., $h^* = \frac{1}{|\mathcal{A}|}\sum_{i\in\mathcal{A}} \widetilde{h}_i$, where $\widetilde{h}_i$ is the critical point of function η_i^d in Eq. (3), i.e., $\nabla\eta_i^d(\widetilde{h}_i) = 0$. Here, η_i^d is the average pathloss between the DBS and location i (i.e., Eq. (3)) and $\nabla\eta_i^d(h) = \frac{d\eta_i^d}{dh}$. In the simulations, we will consider SMBS as the baseline method, and calculate the SE improvement incurred by other three methods (i.e., comparing the SE of the hotspot area incurred by the SMBS to that incurred by STAR, SOAP, STABLE, and CDBS, respectively). Also, to analyze the optimality of STAR, we conduct a brute-force search to find the optimal solution of $\boldsymbol{P0}$. In the brute-force search, the DBS is iteratively placed over a location in a hot spot. For each location, the altitude of the DBS is iteratively selected from $h^{\min}$ to $h^{\max}$ with 2 m increment. For each 3D DBS placement, we calculate the user association and the total SE of the hotspot. The optimal 3D placement of the DBS is the one that incurs the highest SE of the hotspot.

Fig. 2 shows the 3D position of the DBS, the user association, and the SEs of the locations in the hotspot area incurred by SMBS, STAR, SOAP, OPT (i.e., brute-force search), STABLE, and CDBS. STABLE and CDBS assume that the DBS is placed at the center of the hotspot area, but with different altitudes. Since the DBS is placed very close to the MBS and the transmission power of the MBS is much higher than that of the DBS, STABLE and CDBS do not improve the spectral efficiency significantly. As shown in Fig. 2(e), by applying STABLE, only a small number of locations are associated with the DBS. Note that a location is associated with the DBS only if the SE is improved as compared to the location associated with the MBS (i.e., SMBS). Thus, the more locations are associated with the DBS, the more improved the SE of the area can be as compared to SMBS. As shown in Fig. 2(f), no location is associated with the DBS by applying CDBS, and thus the spectral efficiency of the hotspot area is not improved as compared to SMBS. On the other hand, STAR, OPT, and SOAP generate similar DBS locations, which are far away from the MBS to improve the SEs of the locations that are at the edge of the hotspot area. The number of locations associated with the DBS by applying STAR is more than by applying SOAP, but less than by applying OPT. Fig. 3, which

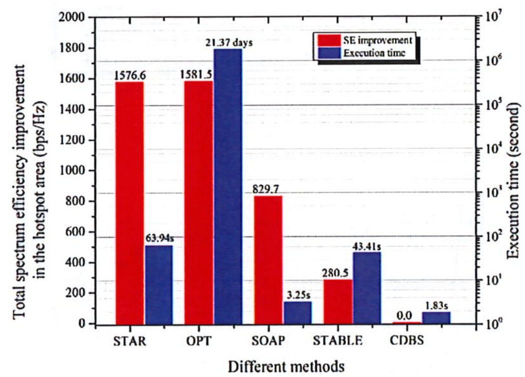

Fig. 3. Total SE improvement and execution time.

shows the total SE improvement (as compared to SMBS) of the whole hotspot area as well as the execution time of different methods, provides more straightforward results to demonstrate the performance. We can see that the total SE improvement incurred by STAR is very close to OPT and much higher than other methods. Meanwhile, the execution time of STAR is much less than OPT (which takes more than 21 days). Although the execution time of STAR is more than SOAP, STABLE, and CDBS, it is feasible to implement STAR in real application scenarios, where the location of a DBS is not frequently updated owing to the slow hotspot movement.

Next, we analyze how the position of the hotspot area affects the performance of different methods. We move the hotspot area from west to east without changing its size, i.e., $\langle 100\sim 700\text{ m}, 300\sim 700\text{ m}\rangle$, $\langle 125\sim 725\text{ m}, 300\sim 700\text{ m}\rangle \ldots$, where the range of the hotspot area in the Y coordinates does not change, but the range of the hotspot area in the X coordinates moves 25 m to the east in each iteration. Fig. 4 shows the total SE improvement incurred by the different methods by varying the position of the hotspot area. Here, the values of the X axis in Fig. 4 refers to the range of the hotspot area in the X coordinates. Fig. 5 shows the 3D DBS position incurred by different methods when the hotspot area is moved from west

[14] H. Tabassum, A. H. Sakr, and E. Hossain, "Massive MIMO-enabled wireless backhauls for full-duplex small cells," in *Proc. IEEE Global Commun. Conf.*, Dec. 2015, pp. 1–6.
[15] M. A. Abdel-Malek, A. S. Ibrahim, M. Mokhtar, and K. Akkaya, "UAV positioning for out-of-band integrated access and backhaul millimeter wave network," *Phys. Commun.*, 2019, Art. no. 100721.
[16] H. Kaushal and G. Kaddoum, "Optical communication in space: Challenges and mitigation techniques," *IEEE Commun. Surv. Tuts.*, vol. 19, no. 1, pp. 57–96, Jan.–Mar. 2017.
[17] I. I. Kim and E. J. Korevaar, "Availability of free-space optics (FSO) and hybrid FSO/RF systems," in *Proc. Opt. Wireless Commun. IV*, vol. 4530, 2001, pp. 84–95.
[18] A. Baid, R. Madan, and A. Sampath, "Delay estimation and fast iterative scheduling policies for LTE uplink," in *Proc. 10th Int. Symp. Model. Optim. Mobile, Ad Hoc Wireless Netw.*, May 2012, pp. 89–96.
[19] N. Ansari and X. Sun, "Mobile edge computing empowers Internet of Things," *IEICE Trans. Commun.*, vol. 101, no. 3, pp. 604–619, 2018.
[20] I. Bor-Yaliniz and H. Yanikomeroglu, "The new frontier in RAN heterogeneity: Multi-tier drone-cells," *IEEE Commun. Mag.*, vol. 54, no. 11, pp. 48–55, Nov. 2016.
[21] B. V. Der Bergh, A. Chiumento, and S. Pollin, "LTE in the sky: Trading off propagation benefits with interference costs for aerial nodes," *IEEE Commun. Mag.*, vol. 54, no. 5, pp. 44–50, May 2016.
[22] A. Al-Hourani, S. Kandeepan, and S. Lardner, "Optimal LAP altitude for maximum coverage," *IEEE Wireless Commun. Lett.*, vol. 3, no. 6, pp. 569–572, Dec. 2014.
[23] M. Alzenad, A. El-Keyi, F. Lagum, and H. Yanikomeroglu, "3-D placement of an unmanned aerial vehicle base station (UAV-BS) for energy-efficient maximal coverage," *IEEE Wireless Commun. Lett.*, vol. 6, no. 4, pp. 434–437, Aug. 2017.
[24] R. I. Bor-Yaliniz, A. El-Keyi, and H. Yanikomeroglu, "Efficient 3-D placement of an aerial base station in next generation cellular networks," in *Proc. IEEE Int. Conf. Commun.*, May 2016, pp. 1–5.
[25] M. M. Azari, F. Rosas, K. Chen, and S. Pollin, "Ultra reliable UAV communication using altitude and cooperation diversity," *IEEE Trans. Commun.*, vol. 66, no. 1, pp. 330–344, Jan. 2018.
[26] A. Ahmed, M. Awais, T. Akram, S. Kulac, M. Alhussein, and K. Aurangzeb, "Joint placement and device association of UAV base stations in IoT networks," *Sensors*, vol. 19, no. 9, 2019, Art. no. 2157.
[27] A. V. Savkin and H. Huang, "Deployment of unmanned aerial vehicle base stations for optimal quality of coverage," *IEEE Wireless Commun. Lett.*, vol. 8, no. 1, pp. 321–324, Feb. 2019.
[28] H. Huang, A. V. Savkin, M. Ding, and M. A. Kaafar, "Optimized deployment of drone base station to improve user experience in cellular networks," *J. Netw. Comput. Appl.*, vol. 144, pp. 49–58, 2019.
[29] H. Huang and A. V. Savkin, "A method for optimized deployment of unmanned aerial vehicles for maximum coverage and minimum interference in cellular networks," *IEEE Trans. Ind. Informat.*, vol. 15, no. 5, pp. 2638–2647, May 2019.
[30] J. Lyu, Y. Zeng, R. Zhang, and T. J. Lim, "Placement optimization of UAV-mounted mobile base stations," *IEEE Commun. Lett.*, vol. 21, no. 3, pp. 604–607, Mar. 2017.
[31] X. Sun and N. Ansari, "Jointly optimizing drone-mounted base station placement and user association in heterogeneous networks," in *Proc. IEEE Int. Conf. Commun.*, May 2018, pp. 1–6.
[32] O. Esrafilian and D. Gesbert, "Simultaneous user association and placement in multi-UAV enabled wireless networks," in *Proc. 22nd Int. ITG Workshop Smart Antennas*, Mar. 2018, pp. 1–5.
[33] Q. Zhang, M. Mozaffari, W. Saad, M. Bennis, and M. Debbah, "Machine learning for predictive on–demand deployment of UAVs for wireless communications," in *Proc. IEEE Global Commun. Conf.*, Dec. 2018, pp. 1–6.
[34] R. Ghanavi, E. Kalantari, M. Sabbaghian, H. Yanikomeroglu, and A. Yongacoglu, "Efficient 3D aerial base station placement considering users mobility by reinforcement learning," in *Proc. IEEE Wireless Commun. Netw. Conf.*, Apr. 2018, pp. 1–6.
[35] W. Khawaja, I. Guvenc, D. W. Matolak, U. Fiebig, and N. Schneckenberger, "A survey of air-to-ground propagation channel modeling for unmanned aerial vehicles," *IEEE Commun. Surv. Tuts.*, vol. 21, no. 3, pp. 2361–2391, Jul.–Sep. 2019.
[36] X. Guo, R. Nkrow, N. Ansari, L. Li, and L. Wang, "Robust WiFi localization by fusing derivative fingerprints of RSS and multiple classifiers," *IEEE Trans. Ind. Informat.*, to be published, doi: 10.1109/TII.2019.2910664.
[37] L. Zhang, Q. Fan, and N. Ansari, "3-D drone-base-station placement with in-band full-duplex communications," *IEEE Commun. Lett.*, vol. 22, no. 9, pp. 1902–1905, Sep. 2018.
[38] E. Kalantari, M. Z. Shakir, H. Yanikomeroglu, and A. Yongacoglu, "Backhaul-aware robust 3D drone placement in 5G+ wireless networks," in *Proc. IEEE Int. Conf. Commun. Workshop*, May 2017, pp. 109–114.
[39] P. Jain *et al.*, "Non-convex optimization for machine learning," *Found. Trends Mach. Learn.*, vol. 10, no. 3-4, pp. 142–336, 2017.
[40] J. Barzilai and J. M. Borwein, "Two-point step size gradient methods," *IMA J. Numer. Anal.*, vol. 8, no. 1, pp. 141–148, 1988.

Xiang Sun (S'13–M'18) received the B.E. and M.E. degrees from the Hebei University of Engineering, Handan, China, in 2008 and 2011, respectively, and the Ph.D. degree in electrical engineering from the New Jersey Institute of Technology, Newark, NJ, USA, in 2018. He is currently an Assistant Professor with the Department of Electrical and Computer Engineering, University of New Mexico, Albuquerque, NM, USA. His research interests include wireless networks, free space optics, Internet of Things, mobile edge computing and networking, big-data-driven networking, and green communications and computing. He was an Associate Editor for *Digital Communications and Networks*.

Nirwan Ansari (S'78–M'83–SM'94–F'09) received the Ph.D. degree from Purdue University, West Lafayette, IN, USA, the M.S.E.E. degree from the University of Michigan, Ann Arbor, MI, USA, and the B.S.E.E. degree (*summa cum laude* with a perfect GPA) from the New Jersey Institute of Technology (NJIT), Newark, NJ, USA. He is currently a Distinguished Professor of electrical and computer engineering with NJIT. He authored *Green Mobile Networks: A Networking Perspective* (IEEE, 2017) with T. Han, and coauthored two other books. He has also authored or coauthored more than 600 technical publications, more than 300 published in widely cited journals/magazines. He has guest-edited a number of special issues covering various emerging topics in communications and networking. He has served on the editorial/advisory board of more than ten journals including as Associate Editor-in-Chief for IEEE WIRELESS COMMUNICATIONS MAGAZINE. His current research focuses on green communications and networking, cloud computing, drone-assisted networking, and various aspects of broadband networks. He was elected to serve in the IEEE Communications Society (ComSoc) Board of Governors as a Member-at-Large, has chaired some ComSoc technical and steering committees, has been serving in many committees such as the IEEE Fellow Committee, and has been actively organizing numerous IEEE International Conferences/Symposia/Workshops. He is frequently invited to deliver keynote addresses, distinguished lectures, tutorials, and invited talks. Some of his recognitions include several excellence in teaching awards, a few best paper awards, the NCE Excellence in Research Award, several ComSoc TC Technical Recognition awards, the NJ Inventors Hall of Fame Inventor of the Year Award, the Thomas Alva Edison Patent Award, Purdue University Outstanding Electrical and Computer Engineering Award, the NCE 100 Medal, NAI Fellow, and designation as a COMSOC Distinguished Lecturer. He has also been granted more than 40 U.S. patents.

Rafael Fierro (S'95–M'98–SM'13) received the M.Sc. degree in control engineering from the University of Bradford, England, U.K. and the Ph.D. degree in electrical engineering from the University of Texas at Arlington. Since 2007, he has been a Professor with the Department of Electrical and Computer Engineering, University of New Mexico, Albuquerque, NM, USA. His current research interests include cyber-physical systems, heterogeneous robotic networks, unmanned aerial vehicles (UAV), and real-time machine learning. The National Science Foundation (NSF), US Department of Defense (DOD), Department of Energy (DOE), and Sandia National Laboratories have funded his research. He directs the AFRL-UNM Agile Manufacturing Center and the Multi-Agent, Robotics, and Heterogeneous Systems (MARHES) Laboratory. Dr. Fierro was the recipient of a Fulbright Scholarship, National Science Foundation CAREER Award, and the 2008 International Society of Automation (ISA) Transactions Best Paper Award. He is an Associate Editor for the IEEE TRANSACTIONS ON AUTOMATION SCIENCE AND ENGINEERING.